Biochimica et Biophysica Acta, 724 (1983) 6–19
Elsevier

BBA 41317

A STRUCTURAL INVESTIGATION OF CYTOCHROME *c* BINDING TO PHOTOSYNTHETIC REACTION CENTERS IN RECONSTITUTED MEMBRANES

JAMES M. PACHENCE [a-d,*], P. LESLIE DUTTON [a] and J. KENT BLASIE [a-c]

[a] *Department of Chemistry,* [b] *Department of Biochemistry/Biophysics, University of Pennsylvania, Philadelphia, PA 1904,* [c] *Department of Biology, Brookhaven National Laboratory, Upton, NY 11974 and* [d] *Department of Biochemistry, Columbia University, College of Physicians and Surgeons, New York, NY 10032 (U.S.A.)*

(Received November 1st, 1982)
(Revised manuscript received March 28th, 1983)

Key words: Photosynthesis; Cytochrome c; Reaction center; Membrane reconstitution; X-ray diffraction; Neutron diffraction

Mammalian cytochrome *c* can effectively replace bacterial cytochrome c_2 as the electron donor to the bacterial photosynthetic reaction center in either the natural chromatophore or a reconstituted reaction center/phospholipid membrane. In this paper, the reconstituted membrane was used to describe the nature of cytochrome *c* binding to the reaction center, the location of bound cytochrome *c* in the membrane profile and the perturbation of the reaction center and phospholipid profile structures induced by cytochrome *c* binding. These structural studies utilized the combined techniques of X-ray and neutron diffraction.

Introduction

The primary events in bacterial photosynthesis occur within the reaction center, an integral membrane protein in the chromatophore membrane. Light absorption by the reaction center bacteriochlorophyll dimer results in an electron transfer from the excited-state dimer to the primary quinone electron acceptor Fe-Q_1, via bacteriopheophtin monomer and bacteriochlorophyll monomer intermediates, within 150 ps [1]. These primary light-induced electron-transfer reactions form the initial segment of a cyclic series of electron-transfer reactions among membrane-associated redox components which is coupled to the synthesis of ATP [2]. Cytochrome c_2 is a peripheral membrane protein which binds electrostatically to the reaction center and functions as the electron donor to the reaction center chlorophyll dimer in this series; the reduction of the dimer by reduced cytochrome c_2 occurs within microseconds following light excitation of the dimer [3]. The electrostatic binding of cytochrome c_2 to the reaction center is associated with a decrease in its redox potential analogous to the binding of cytochrome *c* to cytochrome oxidase in the mitochondrial inner membrane [4]. The bacterial cytochrome c_2 from *Rhodopseudomonas sphaeroides* has a molecular weight and globular shape similar to that of horse heart cytochrome *c* [5]; the small differences in redox potential and surface charge of these two cytochrome *c* molecules do not affect the kinetics of their electron-transfer reaction with the reaction center chlorophyll dimer [3,6].

In previous studies, we have characterized the profile structure (i.e., the average structure along the axis normal to the membrane plane) of the reaction center molecule to approx. 10 Å resolu-

* To whom correspondence should be addressed at: Department of Biochemistry, Columbia University, College of Physicians and Surgeons, 630 W. 168th St., New York, NY 10032, U.S.A.

0005-2728/83/$03.00 © 1983 Elsevier Science Publishers B.V.

tion within a reconstituted reaction center/phospholipid membrane [7]. These reconstituted membranes were fully functional with regard to their primary light-induced electron-transfer reactions and the kinetics of their oxidation of cytochrome *c* electrostatically bound to the reaction centers [8]. The structural studies utilized an essential combination of the techniques of X-ray and neutron diffraction [7–9].

In this paper, we shall describe the nature of cytochrome *c* binding to the reaction centers of these reconstituted membranes. The focus of this paper is the utilization of the combination of X-ray and neutron diffraction techniques to locate the position of cytochrome *c* binding to the reaction center in the membrane profile structure and to provide low-resolution structural information concerning the effect of cytochrome *c* binding on the separate reaction center and phospholipid profile structures. This work has been briefly reported elsewhere [10].

Methods

Reaction centers were prepared from *Rps. sphaeroides* R26 cells according to the method of Clayton and Wang [11]. The index of purity, defined as A_{280}/A_{800}, was measured to be 1.25–1.31 for the reaction centers used in these experiments, with an average purity of 1.27 [12]. Deuterated reaction centers were isolated from bacteria grown on 95% ^2H_2O; these reaction centers were found to be 85% deuterated [7].

Egg phosphatidylcholine (PC) was isolated from fresh egg yolks, as outlined by Singleton, et al. [13]. Reconstituted reaction center/PC unilamellar membrane vesicles were formed according to the methods of Pachence et al. [14]. The oriented membrane multilayers used for the diffraction experiments were made from suspensions of reaction center/PC membrane vesicles with or without electrostatically bound cytochrome *c*, as previously described [14].

Horse heart cytochrome *c* type VII was purchased from Sigma, St. Louis, Mo. It was further purified by using cellulose ion-exchange chromatography (CM 52 from Whatman, Clifton, NJ).

Studies of the binding of cytochrome *c* to reaction center protein were done by sedimentation of a dispersion of the reconstituted membrane vesicles with a known concentration of cytochrome *c*; the cytochrome *c*-membrane complexes were sedimented onto plastic strips in centrifugation cells described previously [8]. The supernatant was removed and the pellet was resuspended in 10 mM Tris-HCl buffer, pH 8; the reduced minus oxidized optical absorption signal at 550 nm ($\Delta\varepsilon = 19.5$ $cm^{-1} \cdot mM^{-1}$) was compared with the reduced minus oxidized signal at 865 nm ($\Delta\varepsilon = 128$ $cm^{-1} \cdot mM^{-1}$) of both the supernatant and the resuspended pellet to determine the amount of bound cytochrome *c* per reaction center. There was no measurable amount of reaction center or PC in the supernatant in all the binding experiments. The lipid-to-protein ratio was obtained by first performing Blye-Dyer extractions on a reaction center/PC suspension to separate protein from phospholipid [15], then measuring lipid phosphate in the chloroform phase [16].

Procedures for the collection, reduction and analysis of the X-ray and neutron diffraction data from the oriented membrane multilayers have been explained previously [7,14].

Results

(A) Equilibrium binding of cytochrome c to reaction center/phospholipid membranes

The binding of mammalian cytochrome *c* to the reconstituted reaction center/phospholipid membranes was investigated using centrifugation to separate the cytochrome *c*-membrane complex from the unbound cytochrome *c*. The method insures that the unbound and bound cytochrome *c* remain in equilibrium throughout the experiment. Oxidized minus reduced optical absorption spectra at 550 nm were recorded to measure the content of unbound cytochrome *c* in the supernatant and the bound cytochrome *c* in the resuspended pellet.

The concentration of reaction center protein was measured in the resuspended pellet as A_{860}, and the availability of the active cytochrome *c*-binding site(s) on the reaction center was determined from single-turnover cytochrome *c* photooxidation kinetics [8]. More than 90% of the photooxidized bacteriochlorophyll dimer was reduced by cytochrome *c* added to preformed vesicles [8]. As a control experiment, cytochrome *c* binding

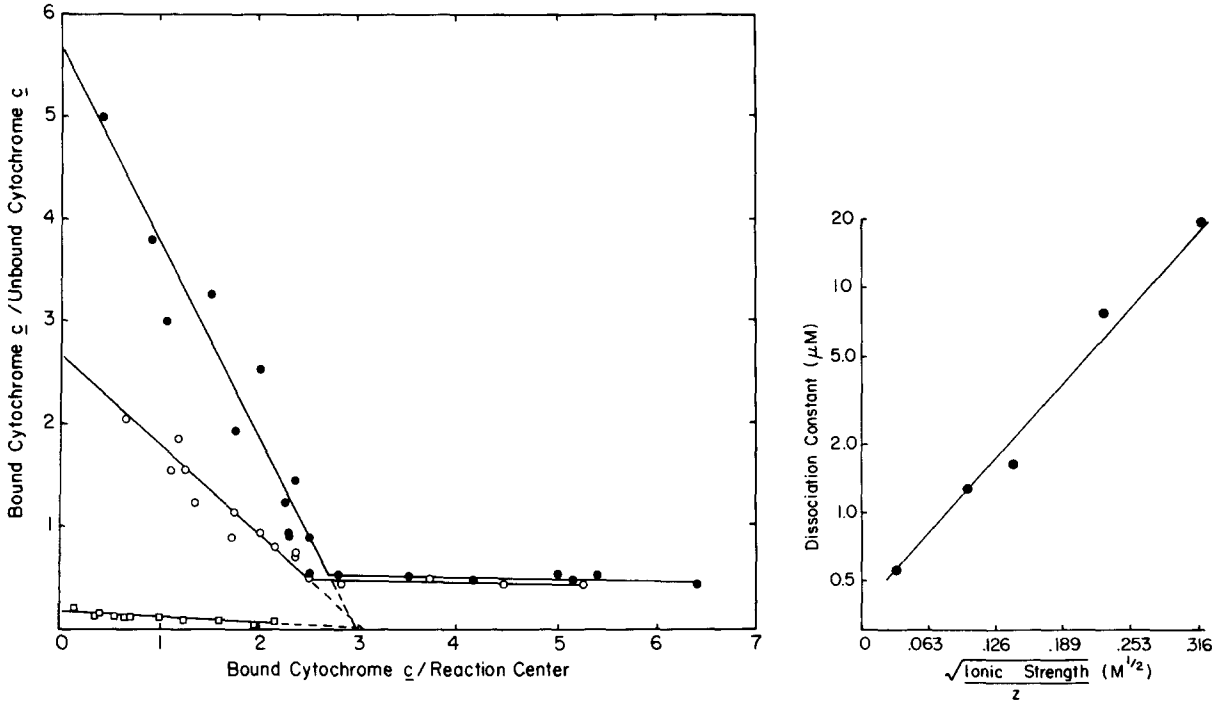

Fig. 1. Equilibrium binding of reduced horse heart cytochrome *c* to reconstituted reaction center/PC membrane vesicles was studied as a function of ionic strength. The lipid/protein mole ratio was approx. 100:1 and the reaction center concentration was 1.30 μM. (A) Scatchard binding plots are shown for three experiments: (●) 1 mM Tris-HCl, (○) 1 mM Tris-HCl with 20 mM KCl, and (□) 1 mM Tris-HCl with 100 mM KCl, all at pH 8.0. (B) The log of the dissociation constant K_D plotted as a function of the square root of ionic strength.

to pure PC membranes was measured, using the same procedure. It was found that binding of cytochrome *c* to pure PC unilamellar vesicles is negligible, and can be ignored (data not shown). Fig. 1A shows the Scatchard binding plots for the cytochrome *c*-reaction center/PC membrane complexes dispersed in buffers having three different ionic strengths. As can be seen, the K_D for the strongly associated cytochrome *c*-reaction center/PC complex increased as the ionic strength increased, but the number of binding sites per reaction center remained invariant at a value of approx. 3. The experimental relationship between the square root of the ionic strength and the logarithm of K_D is approximately linear, as can be seen in Fig. 1B. This implies that the interaction between cytochrome *c* and reaction center/PC membranes can be modelled as an interaction involving two oppositely charged spheres, according to the Debye-Hückel approximation [16]. The isoelectric points for the reaction center and cytochrome *c* at pH 8 are 6.1 and 10.65, respectively, which is consistent with data in Fig. 1 [6].

It was also found that the K_D for cytochrome *c* binding to reaction center/PC membranes was dependent on the redox state of cytochrome *c*; this has been demonstrated by the centrifugation methods as described above [17], and also by redox potentiometry [18]. Cytochrome *c* associated with the reaction center/PC membrane has a lower midpoint potential than either free aqueous cytochrome *c*, cytochrome *c* associated with pure PC membranes, or cytochrome *c* associated with reaction center-detergent complexes [18].

(B) Lamellar X-ray diffraction

The oriented multilayers used in this study were formed from unilamellar dispersions of reaction center/PC membranes and cytochrome *c* such that the bound cytochrome *c*/reaction center ratio in

the multilayer was less than 1. In all experiments, the low ionic strength buffer was 1 mM Tris-HCl (pH 8.0) and the PC/reaction center molar ratio was 100. These partially dehydrated, oriented membrane multilayers were found to be a fully functional liquid-crystalline system. These oriented multilayers provided lamellar X-ray diffraction exhibiting a small mosiac spread (approx. 4° full-width at half-maximum), a negligible degree of lattice disorder and significant diffraction extending to $s = 2\sin\theta/\lambda = 1/9$ Å (Fig. 2 and 3B). Small changes in the relative humidity of the multilayer environment (90–98% relative humidity at 7–8°C) after the initial partial dehydration did not substantially alter these general characteristics of the lamellar diffraction.

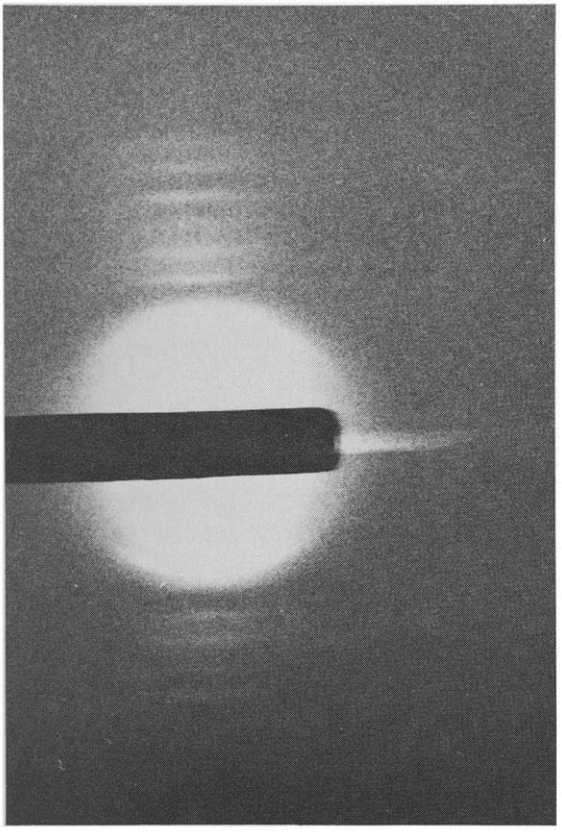

Fig. 2. Lamellar X-ray diffraction patterns are shown from membrane multilayers comprised of PC, reaction center protein, and cytochrome *c* in a mole ratio of 100:1:0.8, respectively. The membrane multilayer used in this experiment was subjected to an atmosphere of 95% relative humidity at 6°C.

The periodicity of reaction center/PC membrane multilayers was 128 Å at 95% relative humidity (Fig. 3A); the periodicity of pure PC membranes under the same conditions was 58 Å [8]. The membrane multilayers containing bound cytochrome *c*/reaction center ratios of less than 1 had periodicities ranging from 130 to 135 Å at 95% relative humidity; the lamellar diffraction shown in Fig. 3B was recorded from a membrane multilayer containing a cytochrome *c*/reaction center ratio of 0.8 and has a periodicity of 132 Å. Multilayers containing cytochrome *c*/reaction center ratios greater than 1 have also been studied and will be presented separately (Pachence, J.M., Dutton, P.L. and Blasie, J.K.; unpublished data). We note (see Fig. 3) that the general characteristics of the lamellar diffraction from the membrane multilayers do not very dramatically with bound cytochrome *c* content for cytochrome *c*/reaction center ratios less than 1. Generally, the lower even-order reflections ($h = 2,4$) are strong, the lower odd-order reflections ($h = 1,3,5$) are weak while the higher order reflections ($h = 6–10$) have comparable intensities. As the cytochrome *c*/reaction center molar ratios increase from 0 to 1, the lower odd-order reflections ($h = 1,3,5$) increase slightly in intensity and the higher order reflections ($h = 6–10$) decrease in intensity as compared to the strong even orders ($h = 2,4$).

As was shown previously, the oriented PC/reaction center membrane multilayers consist predominantly of stacks of flattened unilamellar vesicles [8]. The average orientation of the stacking axis is normal to the multilayer support and the multilayer unit-cell profile contains two asymmetric single-membrane profiles with a mirror plane of symmetry between them. This conclusion was based on the essential characteristics of the lamellar X-ray diffraction and the lamellar neutron diffraction from these oriented multilayers recorded over a range of multilayer periodicities and $H_2O/^2H_2O$ hydration ratios. Since the X-ray and neutron lamellar diffractions from these cytochrome *c*-reaction center/PC membrane multilayers exhibit the same essential characteristics as that from the PC/reaction center membrane multilayers, we conclude that their unit-cell profiles are also centrosymmetric in the profile projection containing the two apposed single-membrane pro-

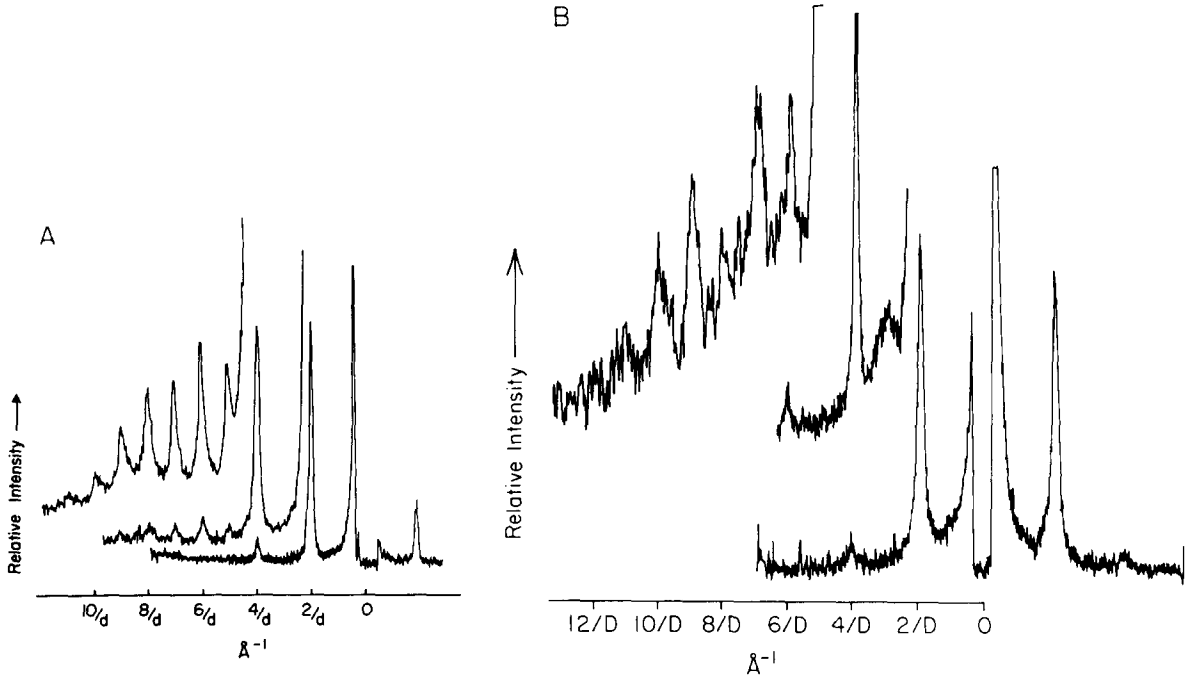

Fig. 3. Microdensitometer traces of the lamellar X-ray diffraction obtained from membrane multilayers consisting of (A) reaction center protein and PC, PC/reaction center = 100 : 1 (mole ratio), with $D = 128$ Å at a relative humidity of 95%, 6°C. (B) Reaction center protein, PC and cytochrome *c*, with PC/reaction center/cytochrome *c* = 100 : 1 : 0.8 (mole ratio), with $D = 132$ Å at a relative humidity of 95%, 6°C.

files of the flattened unilamellar membrane vesicle. Therefore, the phases of the lamellar reflections are limited to 0 or π and the phase problem for the lamellar X-ray reflections was solved by the swelling method using the algorithm of Stamatoff and Krimm [19]. The remaining ambiguity of the overall sign of the thus-derived unit-cell electron-density profiles was resolved by comparing the PC/reaction center single-membrane profiles previously derived and those cytochrome *c*-reaction center/PC single-membrane profiles derived in this study.

The half-unit cell (0 Å $\leqslant x \leqslant D/2$) or single-membrane electron-density profiles for the PC/reaction center membrane and the cytochrome *c*-reaction center/PC membrane are shown in Fig. 4 at approx. 12 Å resolution. We have observed that the structural features within a particular region of the single-membrane profiles, namely, 0 Å $\leqslant x \leqslant 30$ Å, are essentially invariant to variation in the bound cytochrome *c*/reaction center mole ratio over the range 0–3. The obvious changes in the

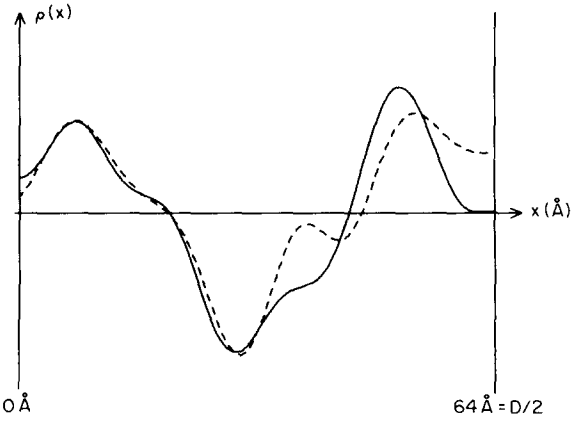

Fig. 4. Unit-cell electron-density profiles were calculated from the lamellar X-ray diffraction patterns (Fig. 3). The single-membrane electron-density profile for PC/reaction center membranes, (———) was superimposed on the single-membrane profile for PC/reaction center/cytochrome *c* membranes (- - - - - -). These two profiles were placed on the same relative scale by finding the best fit ($\rho_1(x) = C * \rho(x)$) in the region of 0 Å $\leqslant |x| \leqslant D/4$ of the two profiles (see text for details).

features of the single-membrane profiles induced by cytochrome *c* binding to the reaction centers vary systematically and are limited to the region 40 Å $\leqslant x \leqslant D/2$ over this range of mole ratios. We could therefore conclude that the bound cytochrome *c* molecule must be located within the half-unit-cell profile within the region 40 Å $\leqslant x \leqslant$ 64 Å. In addition, we could reasonably assume that these single-membrane profiles could be scaled relative to one another such that the best possible least-squares superposition of the profiles occurs over the region 0 Å $\leqslant x \leqslant$ 30 Å. The direct difference profile between the reaction center and reaction center-cytochrome *c* membrane profiles scaled to one another in this manner is shown in Fig. 5.

This direct difference profile might be expected to reveal simply the profile of the bound cytochrome *c* molecule itself if the binding of cytochrome *c* to the reaction center did not perturb the reaction center and/or lipid bilayer profile structure within the membrane. Since the profile structure of cytochrome *c* would be expected to be approximated by a simple step function 25–35 Å in width at this resolution of approx. 12 Å, it is apparent from the unexpected complex features of the difference profile for 35 Å $\leqslant x \leqslant$ 64 Å that some significant perturbation of the reaction center and/or lipid bilayer profile structure has indeed been induced by cytochrome *c* binding to the reaction center. As a result, the neutron diffraction studies described below were undertaken in order to determine directly the nature of these perturbations and the location of cytochrome *c* in the membrane profile.

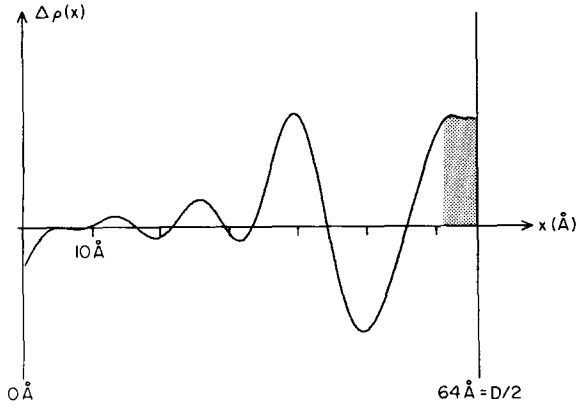

Fig. 5. The difference electron-density profile calculated as the difference between the scaled reaction center/cytochrome *c* and the reaction center single-membrane profiles of Fig. 4. This difference profile clearly shows that cytochrome *c* must be located between 40 Å and *D*/2 in the reaction center/cytochrome *c* single-membrane profile.

(C) Lamellar neutron diffraction

The lamellar neutron diffraction from oriented multilayers composed of cytochrome *c*-reaction center/PC membranes (mole ratio 0.8 : 1.0 : 100, respectively) in which the reaction centers were either protonated or deuterated is shown in Fig. 6. The periodicity of these multilayers was 130 Å. Four lamellar reflections (orders $h = 1$–4) are evident in each case; the relative magnitudes of the various reflections are seen to be strongly dependent on the deuteration of the reaction center. The lamellar diffraction data were collected from these multilayers hydrated with two different H_2O/

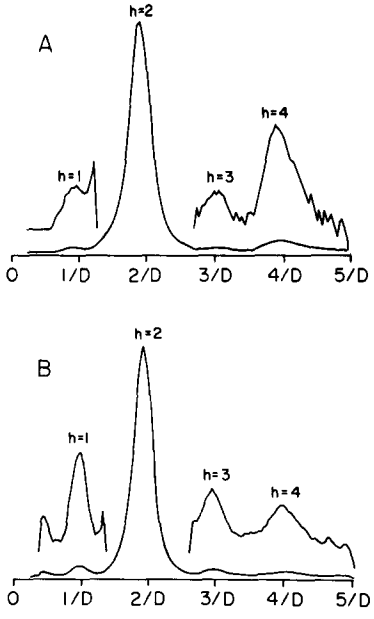

Fig. 6. Lamellar neutron diffraction patterns are shown from partially dehydrated oriented membrane multilayers consisting of (A) protonated PC, protonated cytochrome *c*, and protonated reaction centers in a molar ratio of 100 : 0.8 : 1; and (B) protonated PC, protonated cytochrome *c* and deuterated reaction centers with the same molar ratio of membrane components as in A. The periodicity of the multilayers in A and B was 130 ±0.8 Å at 88% relative humidity, 100% ^2H_2O, 6°C. The inset shows the weaker reflections on a 10-fold expanded scale.

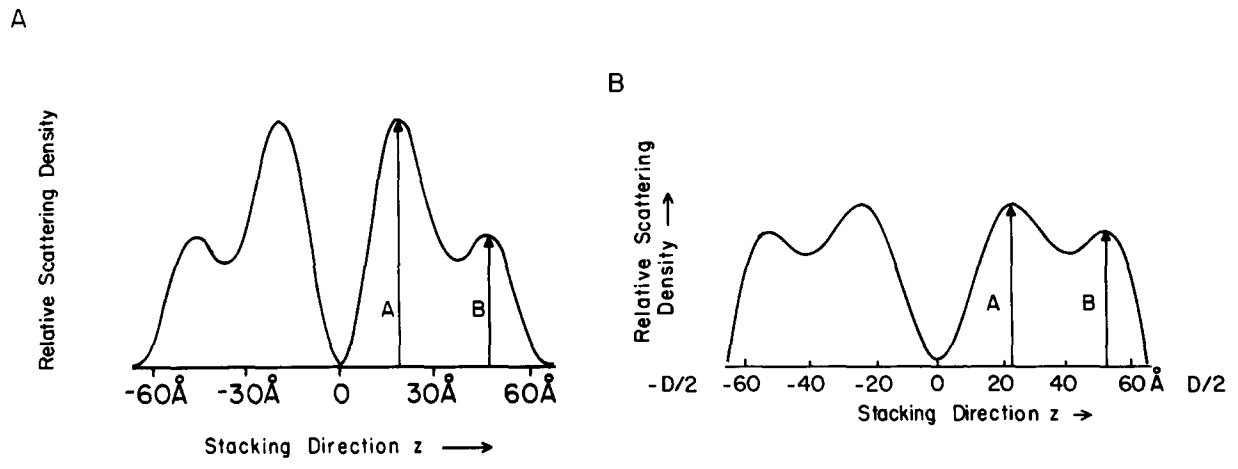

Fig. 7. (A) The reaction center profile calculated by subtracting the scaled protonated reaction center/lipid profile from the scaled deuterated reaction center/lipid profile (no cytochrome *c* present). (B) The reaction center profile calculated by subtracting the scaled protonated reaction center/cytochrome *c*/lipid profile from the scaled deuterated reaction center/cytochrome *c*/lipid profile. The ratio of reaction center protein scattering density within the maxima A and B changed significantly between panels A and B.

^2H_2O ratios (100 and 80% ^2H_2O). The resulting lamellar reflections were phased using a method described in detail previously [20] which utilized the basic fact that the unit-cell water profiles for the protonated and deuterated reaction center membranes must be identical. This phasing procedure also places the total unit-cell neutron scattering profiles for the protonated and deuterated membrane on the same relative scale.

The scaled total unit-cell profile for the protonated reaction-center-cytochrome *c*/PC membrane was subtracted from that for the deuterated reaction center-cytochrome *c*/PC membrane to provide directly the separate reaction center profile shown in Fig. 7A (the reaction center profile within a single-membrane profile is contained within $0\ \text{Å} \leqslant x \leqslant D/2$). This scaled unit-cell reaction center profile and the scaled unit-cell water

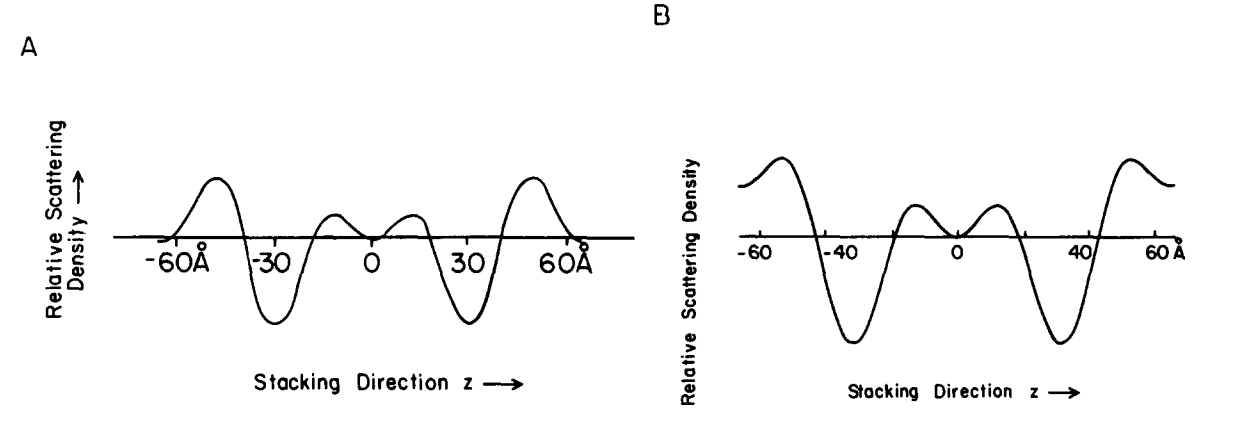

Fig. 8. (A) The lipid scattering density profile, shown on an arbitrary scale, calculated by subtracting the scaled water space profile and the reaction center profile of Fig. 7A from the deuterated reaction center/lipid profile. (B) The cytochrome *c*/lipid profile calculated by subtracting the scaled water space profile and the reaction center profile of Fig. 7B from the deuterated center/cytochrome *c*/lipid profile. The only differences between panels A and B due to the presence of cytochrome *c* occur in the region of 40 $\text{Å} \leqslant |x| \leqslant D/2$.

profile were then subtracted from the total unit-cell neutron scattering profile for the cytochrome *c*-reaction center/PC membrane to provide directly the separate cytochrome *c*-reaction center/PC profile within this membrane as shown in Fig. 8 (again, the contribution of PC and cytochrome *c* to the single-membrane profile is contained within $0\ \text{Å} \leqslant x \leqslant D/2$).

A qualitative comparison of the separate cytochrome *c*/PC profile within the cytochrome *c*-reaction center/PC membrane with the separate PC profile within the reaction center/PC membrane derived previously (see Fig. 8) clearly indicates that major differences between these two profiles occur only within the region $40\ \text{Å} \leqslant x \leqslant D/2$. The location of these differences in the unit-cell profile which must arise from the presence of cytochrome *c* in the separate cytochrome *c*/PC profile is in complete agreement with the independent results of the X-ray diffraction study described above. In order to assess the differences in these low-resolution separate cytochrome *c*/PC and PC profiles on a more quantitative basis, they were subjected to a model refinement analysis.

(D) Model refinement

Model refinement calculations have been used to separate the cytochrome *c* and PC profiles from the cytochrome *c*/PC profile shown in Fig. 8. As outlined in Fig. 9, the low-resolution profile of the separate lipid bilayer was modeled in terms of two step functions of amplitude A and B and width 10 Å whose separation across the bilayer was denoted by the parameter y while the relative amplitude of the two steps was denoted by the parameter $r = A/B$. The parameter y was varied over $30\ \text{Å} \leqslant y \leqslant 35\ \text{Å}$ ($\Delta y = 1.0$ Å) and the parameter r was varied over $0.6 \leqslant r \leqslant 1.2$ ($\Delta r = 0.1$). The low-resolution profile of cytochrome *c* was modeled as a single step function whose width was taken to be approx. 25 Å. This was based on the fact that the structure of horse heart cytochrome *c* is a prolate ellipsoid at low resolution with principal axes of 35 and 25 Å [5] and that the direct difference electron-density profile at approx. 12 Å resolution of Fig. 5 indicates that cytochrome *c* is located within an approx. 25 Å wide region of the cytochrome *c*-reaction center/PC membrane profile. Since the ratio of cytochrome *c* to PC in the membrane multilayer

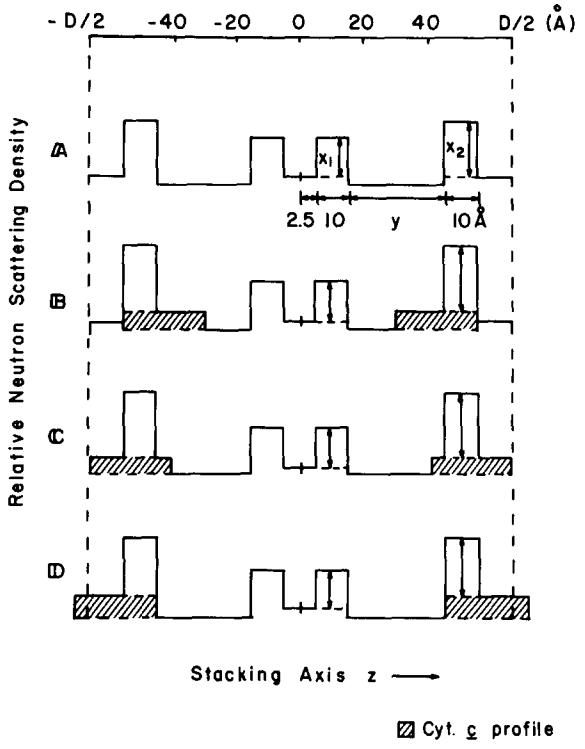

Fig. 9. Step-function model profiles were calculated to represent cytochrome *c*/lipid profile structures within a unit cell having the dimensions of the reaction center/cytochrome *c*/lipid membrane unit-cell profile ($D/2 = 65$ Å). All profile examples are shown as relative neutron scattering density versus position along the membrane profile axis. Model profile A represents an asymmetric lipid profile (no cytochrome *c* contribution), with variable separation between lipid head groups (y), and variable distribution of lipid molecules on opposites sides of the membrane (ratio of x_1/x_2). Model profiles B–D show three examples for the placement of cytochrome *c* (cross-hatched area) relative to the lipid profile. The fit parameters between the experimental structure factors and the calculated model structure factors indicated that panel C represents the most probable model for the cytochrome *c*/lipid profile structure.

is known to better than 5% error, the relative neutron scattering densities of cytochrome *c* and PC were readily calculated, thereby determining the amplitude of the step function representing the cytochrome *c* profile relative to those (A and B) representing the PC profile. Referring to Fig. 9, model A contains no cytochrome *c*. Three model profile projections describing the location of cytochrome *c* within the cytochrome *c*/PC profile were constructed, shown in Fig. 9B–D. Model C con-

tains cytochrome *c* with its center of mass located at $|x| \simeq 52.5$ Å in the membrane profile; in this position, cytochrome *c* extends to the very edge of the unit-cell profile at $|x| = D/2$. Model C is a prime candidate for the cytochrome *c* location in the membrane profile based on a qualitative comparison of the electron-density profiles for the reaction center/PC and cytochrome *c*-reaction center/PC membranes (Fig. 4) which is supported by the separate neutron scattering profiles of Fig. 8. Models B and D contain cytochrome *c* with its center of mass displaced minus 10 Å or plus 5 Å, respectively, relative to the $|x| \simeq 52.5$ Å position of model C. Smaller displacements were not reasonable in terms of the low resolution of the data and the number of variable parameters of the model (see below). We note that in case D (and possibly C), the cytochrome *c* step function shown can belong (i.e., the bound) either to the mebrane contained within $0 \text{ Å} \leqslant x \leqslant D/2$ or to the membrane in the adjacent unit cell contained within $D/2 \leqslant x \leqslant D$ (illustrated in Fig. 9). In the latter case (D), the overlapping of the cytochrome *c* molecules from adjacent membranes in the neighborhood of $|x| \approx D/2$ in the unit-cell profile was properly taken into account in the model refinement calculations described below.

For each of these models, the continuous Fourier transform $F_c(s)$ was calculated and compared with the continuous Fourier transform of the experimentally derived cytochrome *c*/PC profile (Fig. 8) denoted by $F_e(s)$. The comparison utilized the least-squares fit parameter *R* given by:

$$R = \int_0^{s_{max}} [F_c(s) - F_e(s)]^2 ds / \int_0^{s_{max}} [F_e(s)]^2 ds$$

The set of model profiles corresponding to Fig. 9A all provided $R > 0.7$. Since such A-type models fit the separate PC profile within the reaction center/PC membrane extremely well (see Ref. 7), this very poor fit of A-type models to the separate cytochrome *c*/PC profile highlights the significance of the contribution of cytochrome *c* to this profile. The best fit for B-type models was $R = 0.32$ ($r = 0.9$, $y = 34$ Å), for C-type models $R = 0.08$ ($r = 0.9$, $y = 33$ Å) and for D-type models $R = 0.19$ ($r = 1.0$, $y = 33$ Å).

Clearly, this particular C-type model ($r = 0.9$, $y = 33$ Å) represents the best fit of separate cytochrome *c*/PC profile at this resolution. Displacements of the center of mass of the cytochrome *c* profile away from the position $|x| \simeq 52.5$ Å in the unit-cell profile result in significantly poorer fits. We note that modeling the cytochrome *c* profile as a single-step function 35 Å in width (as opposed to 25 Å) resulted in poor fits for all models. It was also found by linear dichroism measurements that the transition moment for the heme optical absorption at 550 nm was parallel to the membrane plane for these oriented membrane multilayers (Pachence, J.M., Blasie, J.K. and Dutton, P.L.; unpublished data). Since this cytochrome *c* heme transition moment is approximately parallel to the major axis of the prolate ellipsoid [5], this result is consistent with the more successful 25 Å step function model of cytochrome *c* used in the model profiles of Fig. 9B–D.

(E) Perturbations induced by cytochrome c binding

In Fig. 7, we compare the separate reaction center profiles within the cytochrome *c*-reaction center/PC membrane (A) and the reaction center/PC membrane (B). The ratio of protein (neutron scattering) density within the peaks denoted 'A' and 'B' (in the figure) changes by more than 40% upon the electrostatic binding of cyto-

TABLE I

TOTAL NEUTRON COUNTS PER BACKGROUND SCATTERING AND LORENTZ-CORRECTED LAMELLAR REFLECTIONS FOR CYTOCHROME *c*-REACTION CENTER/PC MEMBRANES CONTAINING EITHER PROTONATED OR DEUTERATED REACTION CENTERS

Reflection Order	Protonated reaction centers	Deuterated reaction centers
	100% ^2H_2O	100% ^2H_2O
1	401 ± 20 (5.0%)	1110 ± 33 (3.0%)
2	99050 ± 315 (0.3%)	43753 ± 209 (0.5%)
3	819 ± 29 (3.5%)	666 ± 26 (3.9%)
4	4534 ± 67 (1.5%)	604 ± 25 (4.1%)
	75% ^2H_2O	75% ^2H_2O
1	375 ± 19 (5.2%)	731 ± 27 (3.7%)
2	67650 ± 260 (0.4%)	9741 ± 172 (0.6%)
3	396 ± 20 (5.0%)	543 ± 23 (4.3%)
4	2485 ± 50 (2.0%)	456 ± 21 (4.7%)

TABLE II

RESIDUAL ERROR VALUES CALCULATED FROM THE FIT BETWEEN THE WATER SPACE PROFILES OF CYTOCHROME *c*-REACTION CENTER/PC MEMBRANES CONTAINING DEUTERATED OR PROTONATED REACTION CENTER PROTEIN FOR ALL PHASE COMBINATIONS

Phases	+ + + +	+ + + −	+ + − +	− + + +	+ + − −	− + + −	− + − +	− + − −
+ + + +	2.401	> 5	4.012	2.820	> 5	> 5	4.291	> 5
+ + + −	> 5	0.636	> 5	> 5	3.459	4.126	> 5	1.681
+ + − +	4.910	> 5	1.928	> 5	> 5	> 5	> 5	> 5
− + + +	4.041	> 5	> 5	2.290	> 5	> 5	> 5	> 5
+ + − −	> 5	3.370	> 5	> 5	0.938	> 5	> 5	0.320
− + + −	> 5	1.492	> 5	> 5	> 5	0.448	> 5	4.051
− + − +	4.302	> 5	> 5	> 5	> 5	> 5	2.835	> 5
− + − −	> 5	2.820	> 5	> 5	2.440	4.041	> 5	0.272

chrome *c* to the reaction center. This change in the reaction center profile is substantially greater than the experimental errors in the derived reaction center profiles. In Table I, we show the integrated values for the lamellar reflections after correction for background scattering and the Lorentz factor; utilizing the background scattering correction methods described in Ref. 7, the errors in these values are virtually those determined by counting statistics alone. Table II shows the residual error values (see Ref. 7 for details) for the matching of the water space profiles for the two membrane profiles containing either deuterated or protonated reaction centers; the difference between the residual error values of the most probable phase combination pairs is approx. 15%. Since the experimental errors in the measurement of the integrated intensities of the weaker lamellar reflections are approx. 5%, the phase combination pair with the lowest residual value is uniquely determined and the errors in the corresponding reaction center profiles are therefore at the approx. 5% level.

In addition, our previous neutron diffraction study indicated an asymmetry in the separate PC bilayer profile within the reaction center/PC membranes [7]. Model refinement of the separate PC profile using the A-type models of Fig. 9 resulted in an r value of 0.7 for this PC bilayer which corresponds to a 41 : 59 distributional asymmetry in the relative number of PC molecules in the two monolayers of the bilayers; also the separation of the lipid polar head-group peaks across the bilayer was found to be $y = 32$ Å. The fit parameter for the most probable model was $R = 0.10$, comparable to $R = 0.08$ calculated for the model in Fig. 9C. In this study, the electrostatic binding of cytochrome *c* to the reaction center resulted in the separate PC bilayer profile characterized by $r = 0.9$ and $y = 33$ Å (see section D above). This r value corresponds to a distributional asymmetry of 47 : 53 in the relative number of PC molecules in the two monolayers of the bilayer.

Discussion

(A) Characteristics of cytochrome c binding to reaction center / PC membranes

The equilibrium binding experiments indicated that there was a strong interaction between mammalian cytochrome *c* and reaction center protein incorporated into PC membranes, forming a cytochrome *c*-reaction center complex with a K_D of approx. 1 μM. There are two to three cytochrome *c*-binding sites per reaction center depending to the lipid/protein ratio [17]. Only trace amounts of cytochrome *c* were associated with sedimented PC membranes, a result which is supported by previous studies [21]. In addition, previous equilibrium redox titrations of mammalian cytochrome *c* in the presence of reaction center/PC membranes demonstrated differential binding of oxidized and reduced cytochrome *c* to the reaction center by a 40 mV drop in midpoint potential relative to the unbound cytochrome *c*. Redox titrations over a range of protein concentrations indicate dissocia-

tion constants of 0.1 and 0.5 μM for oxidized and reduced cytochrome *c*, respectively, with a total of two binding sites per reaction center [18]; this is in agreement with the equilibrium binding studies previously reported [17]. It has also been shown that the differential binding of oxidized versus reduced cytochrome *c* did not occur with detergent-solubilized reaction centers [22]; detergent-solubilized reaction center protein was reported to have a K_D of 10 μM in one case [6], and another study reported a K_D of 0.4 μM, but only one cytochrome was bound per reaction center and the binding was oxidization state indiscriminate [22].

The oxidation kinetics of cytochrome *c* interacting with the reaction center/PC membranes also supported the notion of a bound cytochrome *c*-reaction center complex. The apparent K_D of the complex calculated from the kinetic experiments was similar to the K_D derived from the equilibrium binding experiments [17]. It is interesting to note that biphasic nature of the oxidation kinetics of cytochrome *c* indicated that there are two functionally separate binding sites on the reaction center [3].

(B) The location of cytochrome c in the membrane profile

The results of the model refinement analysis of the separate neutron cytochrome *c*/PC membrane profile indicated that the center of mass of cytochrome *c* was located at $|x| \approx 47-53$ Å within the single-membrane profile. Cytochrome *c* center of mass locations 5 Å or more away from this 47–53 Å region were significantly inconsistent with the separate cytochrome *c*/PC profile. This location for cytochrome *c* in the membrane profile is also completely consistent with the electron-density profiles at approx. 10 Å resolution for the reaction center/PC and cytochrome *c*-reaction center/PC membranes derived from the X-ray diffractions data.

The most probable position of the cytochrome *c* profile relative to the reaction center profile is shown in Fig. 10. The cytochrome *c*, reaction center and phospholipid structures within these cytochrome *c*-reaction center/PC membranes are shown on an absolute scale schematically in Fig. 10. There is, however, another interpretation of the cytochrome *c* position with respect to the reaction

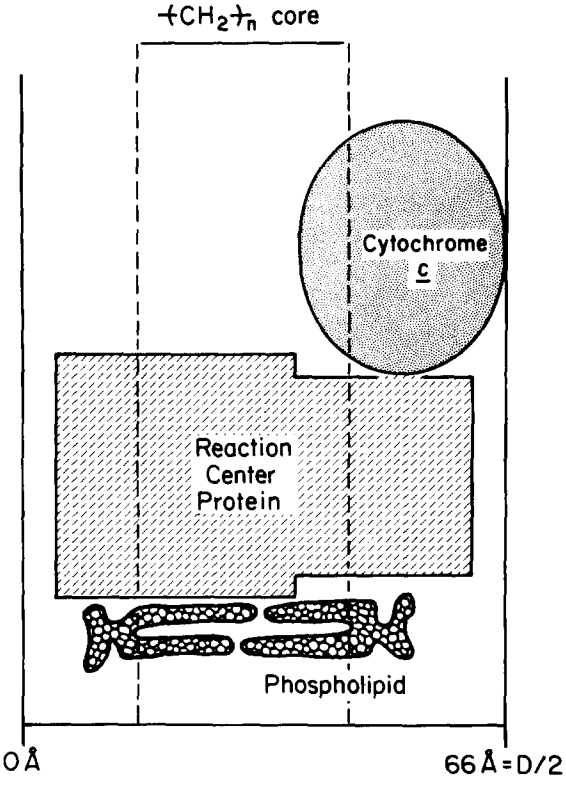

Fig. 10. A schematic representation of the membrane consisting of cytochrome *c* bound to reaction centers in a PC bilayer for cytochrome *c*/reaction center mole ratios ≤ 1. The various components are drawn to scale. The reaction center protein molecule is shown as being symmetric about an axis perpendicular to the membrane plane, as the information obtained from the lamellar diffraction data is cylindrically averaged about this axis. Cytochrome *c* is approximated as a prolate ellipsoid with dimensions of $25 \times 25 \times 35$ Å; evidence presented in this paper indicated that the major axis is parallel to the membrane plane.

center, using the same cytochrome *c* profile distribution. Fig. 11 illustrates that the cytochrome *c* could bind to the reaction center within the same unit cell, or bind to the reaction center in the opposition unit cell. We would favor the first possibility, given the rapid oxidation kinetics of this membrane system [3,6,17] and strong ionic binding [17,18], but the second case is not ruled out. It is interesting to note that this positioning of cytochrome *c* in the membrane profile results in the substantial penetration of cytochrome *c* into the membrane surface to the very edge of the lipid hydrocarbon core. This deep penetration of cytochrome *c* into the reaction center/PC membrane

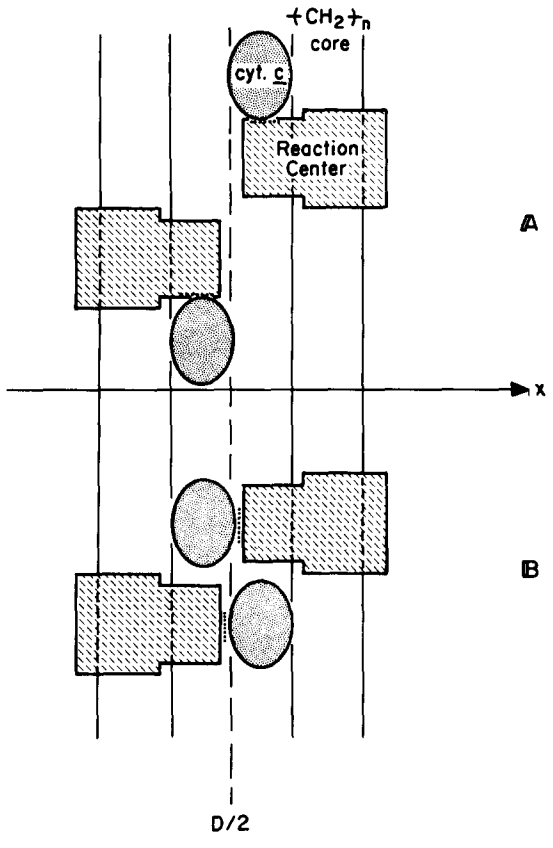

Fig. 11. A schematic representation to illustrate the ambiguity in the cytochrome *c* position with respect to the reaction center. (A) The cytochrome *c* molecule is bound to the reaction center within the same unit cell; (B) the cytochrome *c* molecule is bound to the reaction center in the apposing unit cell. As can be seen, both arrangements have the same distribution of cytochrome *c* in the unit-cell profile projection.

surface explains the relatively small increase in multilayer periodicity (2–5 Å) and also very possibly the redistribution of PC molecules in the lipid bilayer profile upon the electrostatic binding of cytochrome *c* to the reaction center (see section C below).

(C) Cytochrome c perturbation of reaction center/PC membrane structure

As described in Results, the electrostatic binding of cytochrome *c* to the reaction center in these reconstituted reaction center/PC membranes induces a significant perturbation of both the reaction center and phospholipid bilayer profile structures.

The alteration of the reaction center profile could be due either to (a) a significant change in the reaction center molecular profile itself (due to induced structural changes within the reaction center subunits and/or a shift in the relative positions of the subunits) or (b) a significant change in the vectorial distribution of reaction center molecules in the membrane profile. However, it was determined by cytochrome *c* photooxidation kinetics that the reaction centers in the cytochrome *c*-reaction center/PC membranes are vectorially oriented in the membrane profile with $90 \pm 5\%$ of their cytochrome *c*-binding sites facing the extravesicular water space [8]. Therefore, in the presence of cytochrome *c*, the reaction center protein distribution is highly asymmetric as determined kinetically. If vectorial redistribution did occur, then the kinetic results imply that the reaction center profile must be more asymmetric in the presence of cytochrome than in the absence. However, upon inspection of the structural results of Fig. 7, the opposite change in asymmetry occurs, which by elimination would support the first possibility (a).

The alteration in the phospholipid bilayer profile is primarily due to a significant redistribution in the relative number of lipid molecules in each monolayer of the bilayer. This redistribution ('flip-flop' [23]) must occur during the establishment of the cytochrome *c* binding equilibrium with the reaction centers in the membrane.

It would appear that both the strength and site of the electrostatic interaction of cytochrome *c* on the reaction center surface and the cytochrome *c* binding induced change in the reaction center profile structure may be responsible for the redistribution ('flip-flop') of lipid molecules in the bilayer profile. In the former case, the position of the bound cytochrome *c* in the membrane profile would tend to displace phospholipid head groups from the extravesicular surface of the membrane. In the latter case, the more symmetric reaction center profile resulting from cytochrome *c* binding would require less compensatory asymmetry in the lipid bilayer profile.

(D) Comment on the combined X-ray and neutron diffraction approach

We initially expected that the position of cyto-

chrome *c* in the cytochrome *c*-reaction center/PC membrane profile could be reliably determined via the derivation of electron-density profiles at moderate resolution (approx. 10 Å) for these membranes as a function of the cytochrome *c*/reaction center mole ratio. Appropriate direct difference profiles (Fig. 5) were expected to reveal simply the separate cytochrome *c* profile within these membrane profiles. However, it became clear to us from such studies that the systematic variation of the cytochrome *c*/reaction center mole ratio over the range 0–3 induced nontrivial systematic perturbations of the reaction center/PC profile structure within these cytochrome *c*-reaction center/PC membranes. As a result, it became absolutely essential to be able to alter the scattering contrast of selected membrane components (e.g., deuteration for neutron diffreaction) at a constant membrane composition in order to determine accurately the separate molecular profiles of the various components within the total membrane profile.

Therefore, we note that the elucidation of the structural nature of the second cytochrome *c*-binding site on the reaction center for cytochrome *c*/reaction center mole ratios greater than 1.0 will similarly require neutron diffraction studies utilizing deuterated reaction centers and deuterated cytochrome *c*.

Finally, it is important to note that the direct difference electron-density profile between the cytochrome *c*-reaction center/PC and reaction center/PC membrane profiles at approx. 10 Å resolution (see Fig. 7) can be fully predicted within experimental error utilizing the 10 Å resolution reaction center and phospholipid profiles previously calculated [7] as appropriately modified by the results of this study and a 25 Å wide step function model of the cytochrome *c* molecular profile correctly placed within the single-membrane profile (i.e., with its center of mass at $|x| \simeq 52$ Å). These 'appropriate modifications' include only the changes in the reaction center and lipid bilayer profile structures induced by the electrostatic binding of cytochrome *c* to the reaction centers in these membranes as described in section E of Results. The resulting reaction center profile and cytochrome *c* profile within the cytochrome *c*-reaction center/PC membrane profile are shown at approx. 10 Å resolution in Fig. 12.

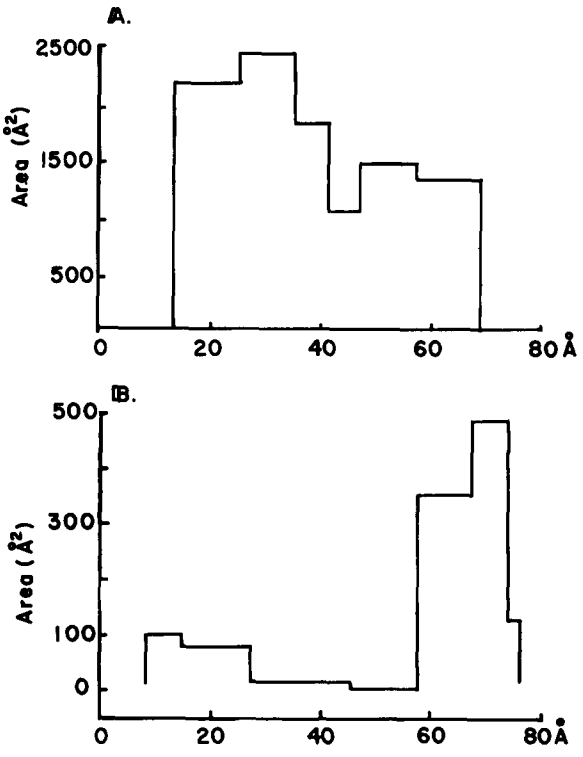

Fig. 12. (A) The 10 Å model molecular area profile of the reaction center protein, as it appears in the reaction center/phospholipid/cytochrome *c* membrane. (B) The 10 Å model area profile of cytochrome *c* distribution within a reaction center/phospholipid/cytochrome *c* membrane. This figure represents half of a unit cell (one asymmetric membrane).

References

1 Kaufmann, K.J., Dutton, P.L., Netzel, T.L., Leigh, J.S. and Rentzepis, P.M. (1975) Science 188, 1301–1304
2 Frankel, A.W. (1954) J. Am. Chem. Soc. 76, 55–85
3 Dutton, P.L., Petty, K.M., Bonner, H.S. and Morse, S.D. (1975) Biochim. Biophys. Acta 387, 536–556
4 Dutton, P.L., Wilson, D.F. and Lee, C.P. (1971) Biochemistry 9, 5077
5 Dickerson, R.E. and Timkovich, R. (1975) in The Enzymes (Boyer, P.D., ed.), 3rd edn., Vol. 2, ch. 7, pp. 395–544, Academic Press, New York
6 Overfield, R.E. and Wraight, C.A. (1980) Biochemistry 19, 3322–3327
7 Pachence, J.M., Dutton, P.L. and Blasie, J.K. (1981) Biochim. Biophys. Acta 635, 267–283
8 Pachence, J.M., Dutton, P.L. and Blasie, J.K. (1979) Biochim. Biophys. Acta 548, 348–373
9 Herbette, L., Scarpa, A., Blasie, J.K., Bauer, D.R., Wang, C.T. and Fleischer, S. (1981) Biophys. J. 36, 27–46
10 Pachence, J.M., Dutton, P.L. and Blasie, J.K. (1982) Biophys. J. 37, 148a

11 Clayton, R.K. and Wang, R.T. (1971) Methods Enzymol. 23, 696–704
12 Okamura, M.Y., Steiner, L.A. and Feher, G. (1974) Biochemistry 13, 1394–1402
13 Singleton, W.S., Gray, M.S., Brown, M.C. and White, J.L. (1965) J. Am. Oil. Chem. Soc. 42, 53–63
14 Blight, E.G. and Dyer, W.J. (1959) Can. J. Biochem. Phys. 37, 911–917
15 Bartlett, G.R. (1959) J. Biol. Chem. 234, 466–468
16 Tanford, C. (1961) Physical Chemistry of Macromolecules, Wiley, New York
17 Pachence, J.M., Moser, C.C., Blasie, J.K. and Dutton, P.L. (1979) Biophys. J. 22, 55a (Abstr.)
18 Moser, C.C., Pachence, J.M., Blasie, J.K. and Dutton, P.L. (1982) Biophys. J. 37, 225a (Abstr.)
19 Stamatoff, J. and Krim, S. (1973) Biophys. J. 16, 503–516
20 Schoenborn, B.P. and Blasie, J.K. (1975) 5th International Biophysics Congress, Villaden and Christensen, Copenhagen, pp. 1379–1381
21 Kimelberg, A.K., Lee, C.P., Claude, A. and Mrena, E. (1970) J. Membrane Biol. 2, 235–251
22 Rosen, D., Okamura, M.Y. and Feher, G. (1980) Biochemistry 19, 5687–5692
23 Op den Kamp, J.A.F. (1979) Annu. Rev. Biochem. 48, 47–71